Adaptive Super Twisting Controller for a Quadrotor UAV

Sujit Rajappa[1], Carlo Masone[1], Heinrich H. Bülthoff[1,2] and Paolo Stegagno[1]

***Abstract*— In this paper we present a robust quadrotor controller for tracking a reference trajectory in presence of uncertainties and disturbances. A Super Twisting controller is implemented using the recently proposed gain adaptation law [1], [2], which has the advantage of not requiring the knowledge of the upper bound of the lumped uncertainties. The controller design is based on the regular form of the quadrotor dynamics, without separation in two nested control loops for position and attitude. The controller is further extended by a feedforward dynamic inversion control that reduces the effort of the sliding mode controller. The higher order quadrotor dynamic model and proposed controller are validated using a SimMechanics physical simulation with initial error, parameter uncertainties, noisy measurements and external perturbations.**

I. INTRODUCTION

In the past decade we have witnessed to the blooming of aerial robotics as a research domain. Unmanned Aerial Vehicles (UAVs) are increasingly used in industrial and civilian applications because their mobility makes them capable to access dangerous areas both in indoor and outdoor scenarios and to tackle a wide variety of tasks. Initially the focus of research was on navigation tasks (mapping, surveillance, etc.), but recently the attention has shifted more towards physical interaction with the environment and manipulation of objects [3], [4], [5], [6], [7], [8].

From this shift towards physical interaction it is emerging the need to have not only good accuracy in trajectory tracking but also robustness to perturbations, such as external disturbances (e.g.: wind gusts) and model uncertainties (e.g.: change in mass when grasping an object).

Indeed, classical control approaches such as nonlinear dynamic inversion and feedback linearization [9] are known for their vulnerability to model uncertainties [10]. Sliding mode control [11] appears to be a promising solution to deal with model uncertainties because it has well known perturbations rejection properties [12]. Yet, this control strategy is also known to suffer from chattering which might reduce the performance and degrade the actuators. In order to overcome this problem, adaptive sliding mode strategies have been proposed both for quadrotors [13] and for fixed wing aircrafts [14].

All the cited control approaches have some limitations. While the controller proposed in [13] still suffers from chattering, [10] shows limited robustness to parameter uncertainties, and [11] requires the knowledge of the upper bound on perturbations which in most practical cases is impossible to estimate, therefore leading to over-conservative tunings. Taking into account all the limitations mentioned above, in this paper we implement an Adaptive Super Twisting Controller (ASTC) with the following properties:

1) It considers and compensates for all the uncertainties (parametric, model, disturbances) lumped together.
2) It does not require any knowledge of the upper bound of the uncertainties.
3) It adapts the gains rather than the model parameter [1]. In this way, the gains are lowered whenever possible, thus reducing control actions, chattering and noise amplification.
4) It uses a feedforward dynamic inversion (FF) to reduce the discontinuous control, thus improving performance and further reducing chattering.

The rest of the paper is organized as follows. We introduce the preliminary system description along with the modeling and adaptation model for control in Sec. II. Then in Sec. III we describe the adaptive super twisting controller. In Sec. IV we validate the controller and the model adaptation by means of physical simulations. Conclusions and future perspectives are discussed in Sec. V.

II. PRELIMINARY SYSTEM DESCRIPTIONS

The quadrotor is a popular configuration of UAV, with four coplanar propellers. Having six degrees of freedom (full 3D pose) and four control inputs (the propellers) it is an under-actuated mechanical system. In this section we introduce the quadrotor model and define the system dynamics in regular form which will be used to design the controller.

A. Dynamic System Model

Let us define the world inertial frame as $\mathcal{F}_W : \{\boldsymbol{O}_W, \boldsymbol{X}_W, \boldsymbol{Y}_W, \boldsymbol{Z}_W\}$ and the body frame attached to the quadrotor as $\mathcal{F}_B : \{\boldsymbol{O}_B, \boldsymbol{X}_B, \boldsymbol{Y}_B, \boldsymbol{Z}_B\}$, where $\boldsymbol{O}_B$ coincides with the quadrotor Center of Mass (CoM). $\mathcal{F}_B$ follows the NED (North-East-Down) convention. Let $\boldsymbol{p} = \begin{bmatrix} x & y & z \end{bmatrix}^T \in \mathbb{R}^3$ describe the position of $\boldsymbol{O}_B$ in $\mathcal{F}_W$ and let $\boldsymbol{\Theta} = \begin{bmatrix} \phi & \theta & \psi \end{bmatrix}^T \in \mathbb{R}^3$ be the standard roll, pitch and yaw angles respectively which describe the orientation of $\mathcal{F}_B$ in $\mathcal{F}_W$, with $\phi, \theta \in [-\pi/2, \pi/2]$ and $\psi \in [0, 2\pi]$. The basic quadrotor states are therefore

$$\begin{bmatrix} \boldsymbol{p}^T & \boldsymbol{\Theta}^T \end{bmatrix}^T = \begin{bmatrix} x & y & z & \phi & \theta & \psi \end{bmatrix}^T \tag{1}$$

[1]Autonomous Robotics and Human-Machine Systems Group. Max Planck Institute for Biological Cybernetics, Spemannstraße 38, 72076 Tübingen, Germany, {sujit.rajappa} {carlo.masone} {hhb} {paolo.stegagno}@tuebingen.mpg.de

[2]Department of Brain and Cognitive Engineering, Korea University, Anam-dong, Seongbuk-gu, Seoul, 136-713 Korea.

Preprint - final, definitive version available at http://www.ieeexplore.com/ accepted for ICRA2016 May 2016

Let $\boldsymbol{R}_{\boldsymbol{\Theta}} = \boldsymbol{R}_z(\psi)\boldsymbol{R}_y(\theta)\boldsymbol{R}_x(\phi) \in \mathbb{R}^{3\times3}$ represent the transformation from $\mathcal{F}_B$ to $\mathcal{F}_W$:

$$\boldsymbol{R}_{\boldsymbol{\Theta}} = \begin{pmatrix} c_\psi c_\theta & c_\psi s_\theta s_\phi - s_\psi c_\phi & c_\psi s_\theta c_\phi + s_\psi s_\phi \\ s_\psi c_\theta & s_\psi s_\theta s_\phi + c_\psi c_\phi & s_\psi s_\theta c_\phi - c_\psi s_\phi \\ -s_\theta & c_\theta s_\phi & c_\theta c_\phi \end{pmatrix} \tag{2}$$

where $c_\star = \cos(\star)$, $s_\star = \sin(\star)$ and $\boldsymbol{R}_z$, $\boldsymbol{R}_y$, $\boldsymbol{R}_x$ denote the 3×3 fundamental rotation matrices around the Z, Y and X axes respectively.

To reduce the complexity of the arising quadrotor model, we consider the following standard assumptions:

Assumption 1: $\mathcal{F}_B$ is aligned with the principal axes of the quadrotor.

Assumption 1 ensures that the inertial matrix $\boldsymbol{I}_B$ is diagonal.

Assumption 2: The inertial and gyroscopic effects arising from propellers and the motors are rejected by the feedback nature of the controller considering them as second-order disturbances.

With the above mentioned assumptions and utilizing the standard Newton-Euler equations of motion, the dynamical equations corresponding to the transational and rotational dynamics of the quadrotor can be written as [15]

$$m\ddot{\boldsymbol{p}} = mge_3 - \rho\boldsymbol{R}_{\boldsymbol{\Theta}}e_3 + \boldsymbol{f}_{\text{ext}} \tag{3}$$

$$\boldsymbol{I}_B\dot{\boldsymbol{\omega}}_B = -\boldsymbol{\omega}_B \times \boldsymbol{I}_B\boldsymbol{\omega}_B + \boldsymbol{\tau} + \boldsymbol{\tau}_{\text{ext}} \tag{4}$$

$$\dot{\boldsymbol{\Theta}} = \boldsymbol{T}(\boldsymbol{\Theta})\boldsymbol{\omega}_B \tag{5}$$

where m is the mass of the quadrotor, $e_3 = \begin{bmatrix}0 & 0 & 1\end{bmatrix}^T$ is the standard $\boldsymbol{Z}_W$-axis representation from NED directions, g is the acceleration due to gravity, $\ddot{\boldsymbol{p}} = \begin{bmatrix}\ddot{x} & \ddot{y} & \ddot{z}\end{bmatrix}^T$ is the acceleration of the quadrotor in $\mathcal{F}_W$, ρ is the thrust control input generated by the propellers along e_3 in $\mathcal{F}_B$, $\boldsymbol{f}_{\text{ext}} = \begin{bmatrix}f_{\text{ext}_x} & f_{\text{ext}_y} & f_{\text{ext}_z}\end{bmatrix}^T \in \mathbb{R}^3$ is the external force acting on the quadrotor in $\mathcal{F}_W$, $\dot{\boldsymbol{\omega}}_{\boldsymbol{B}} = \begin{bmatrix}\dot{p} & \dot{q} & \dot{r}\end{bmatrix}^T \in \mathbb{R}^3$ is the angular acceleration of the quadrotor w.r.t. $\mathcal{F}_B$, $\boldsymbol{\tau} = \begin{bmatrix}\tau_x & \tau_y & \tau_z\end{bmatrix}^T \in \mathbb{R}^3$ is the input moment expressed in $\mathcal{F}_B$, $\boldsymbol{T}(\boldsymbol{\Theta}) \in \mathbb{R}^{3\times3}$ is the transformation matrix from $\boldsymbol{\omega}_B \in so(3)$ to the Euler angle rates $\dot{\boldsymbol{\Theta}}$ and $\boldsymbol{\tau}_{\text{ext}} = \begin{bmatrix}\tau_{\text{ext}_x} & \tau_{\text{ext}_y} & \tau_{\text{ext}_z}\end{bmatrix}^T \in \mathbb{R}^3$ is the external moment that is acting on the quadrotor.

Equations (3)−(5), can be written in state-space form as explained in [9]:

$$\dot{\boldsymbol{x}} = \boldsymbol{f}(\boldsymbol{x}) + \boldsymbol{g}(\boldsymbol{x})\boldsymbol{u} \tag{6}$$

where

$$\boldsymbol{x} = \begin{bmatrix}x & y & z & \phi & \theta & \psi & \dot{x} & \dot{y} & \dot{z} & p & q & r\end{bmatrix}^T \in \mathbb{R}^{12\times1} \tag{7}$$

$$\boldsymbol{f}(\boldsymbol{x}) = \begin{bmatrix} \dot{x} \\ \dot{y} \\ \dot{z} \\ f_{(4,1)} \\ f_{(5,1)} \\ f_{(6,1)} \\ 0 \\ 0 \\ g \\ \frac{Iy-Iz}{Ix}qr \\ \frac{Iz-Ix}{Iy}pr \\ \frac{Ix-Iy}{Iz}pq \end{bmatrix}, \boldsymbol{g}(\boldsymbol{x}) = \begin{bmatrix} 0 & 0 & 0 & 0 \\ 0 & 0 & 0 & 0 \\ 0 & 0 & 0 & 0 \\ 0 & 0 & 0 & 0 \\ 0 & 0 & 0 & 0 \\ 0 & 0 & 0 & 0 \\ g_{(7,1)} & 0 & 0 & 0 \\ g_{(8,1)} & 0 & 0 & 0 \\ g_{(9,1)} & 0 & 0 & 0 \\ 0 & \frac{1}{Ix} & 0 & 0 \\ 0 & 0 & \frac{1}{Iy} & 0 \\ 0 & 0 & 0 & \frac{1}{Iz} \end{bmatrix} \tag{8}$$

$$\boldsymbol{u} = \begin{bmatrix} u_1 \\ u_2 \\ u_3 \\ u_4 \end{bmatrix} = \begin{bmatrix} \rho \\ \tau_x \\ \tau_y \\ \tau_z \end{bmatrix} \tag{9}$$

with

$$\begin{cases} f_{(4,1)} = p + q\sin\phi\tan\theta + r\cos\phi\tan\theta \\ f_{(5,1)} = q\cos\phi - r\cos\phi \\ f_{(6,1)} = q\sin\phi\sec\theta + r\cos\phi\sec\theta \\ g_{(7,1)} = -\frac{1}{m}\left(\cos\phi\cos\psi\sin\theta + \sin\phi\sin\psi\right) \\ g_{(8,1)} = -\frac{1}{m}\left(\cos\phi\sin\psi\sin\theta - \sin\phi\cos\psi\right) \\ g_{(9,1)} = -\frac{1}{m}\left(\cos\phi\cos\theta\right). \end{cases}$$

With respect to the control input (9), we make the following assumption:

Assumption 3: The control input is bounded, i.e., $\boldsymbol{u} \in \mathcal{U} = \{\boldsymbol{u}^\star \in [\boldsymbol{u}_{min}, \boldsymbol{u}_{max}]\}$.

It is well known that the control input in (9) is related to the speed of the propellers. Hence, Assumption 3 implies that the speed of the propellers is always feasible.

B. Regular Control Form

It is well known that the quadrotor is dynamically feedback linearizable with output

$$\boldsymbol{y} = \boldsymbol{h}(\boldsymbol{x}) = \begin{bmatrix}x & y & z & \psi\end{bmatrix}^T. \tag{10}$$

Namely, we can transform (6)−(9) into a non-interacting system as shown in [9]. First, let us introduce a new control input, i.e, $\bar{\boldsymbol{u}}$

$$\bar{\boldsymbol{u}} = \begin{bmatrix} \ddot{u}_1 \\ u_2 \\ u_3 \\ u_4 \end{bmatrix} = \begin{bmatrix} \bar{u}_1 \\ u_2 \\ u_3 \\ u_4 \end{bmatrix} \tag{11}$$

obtained by considering a dynamic extension of (6). Here $\bar{u}_1$ is obtained by the double differentiation of u_1 as,

$$u_1 = \varrho, \tag{12a}$$

$$\dot{\varrho} = \varsigma, \tag{12b}$$

$$\dot{\varsigma} = \bar{u}_1. \tag{12c}$$

The new extended system will have the form

$$\dot{\bar{\boldsymbol{x}}} = \boldsymbol{f}(\bar{\boldsymbol{x}}) + \boldsymbol{g}(\bar{\boldsymbol{x}})\bar{\boldsymbol{u}} \tag{13}$$

where the extended state is

$$\bar{\boldsymbol{x}} = \begin{bmatrix} x & y & z & \phi & \theta & \psi & \dot{x} & \dot{y} & \dot{z} & \varrho & \varsigma & p & q & r \end{bmatrix}^T \in \mathbb{R}^{14\times 1} \tag{14}$$

and

$$\boldsymbol{f}(\bar{\boldsymbol{x}}) = \begin{bmatrix} \dot{x} \\ \dot{y} \\ \dot{z} \\ f_{(4,1)} \\ f_{(5,1)} \\ f_{(6,1)} \\ g_{(7,1)}\varrho \\ g_{(8,1)}\varrho \\ g + g_{(9,1)}\varrho \\ \varsigma \\ 0 \\ \frac{Iy-Iz}{Ix}qr \\ \frac{Iz-Ix}{Iy}pr \\ \frac{Ix-Iy}{Iz}pq \end{bmatrix}, \boldsymbol{g}(\bar{\boldsymbol{x}}) = \begin{bmatrix} 0 & 0 & 0 & 0 \\ 0 & 0 & 0 & 0 \\ 0 & 0 & 0 & 0 \\ 0 & 0 & 0 & 0 \\ 0 & 0 & 0 & 0 \\ 0 & 0 & 0 & 0 \\ 0 & 0 & 0 & 0 \\ 0 & 0 & 0 & 0 \\ 0 & 0 & 0 & 0 \\ 0 & 0 & 0 & 0 \\ 1 & 0 & 0 & 0 \\ 0 & \frac{1}{Ix} & 0 & 0 \\ 0 & 0 & \frac{1}{Iy} & 0 \\ 0 & 0 & 0 & \frac{1}{Iz} \end{bmatrix}. \tag{15}$$

Finally, there exists a diffeomorphism $\Phi(\bar{\boldsymbol{x}})$ such that the coordinates transformation $\boldsymbol{z} = \Phi(\bar{\boldsymbol{x}})$ defined by

$$\begin{cases} z_1 = x, & z_2 = \dot{x}, & z_3 = \ddot{x}, & z_4 = \dddot{x}, \\ z_5 = y, & z_6 = \dot{y}, & z_7 = \ddot{y}, & z_8 = \dddot{y}, \\ z_9 = z, & z_{10} = \dot{z}, & z_{11} = \ddot{z}, & z_{12} = \dddot{z}, \\ & z_{13} = \psi, & z_{14} = \dot{\psi} \end{cases} \tag{16}$$

transforms (13) into a regular form in which the dynamics of the output $\boldsymbol{y}$ in (10) are decoupled into a chain of integrators. The system transformation with the new states $z = [z_1, z_2, \ldots.., z_{14}]^T$ can be written in state-space form as

$$\dot{\boldsymbol{z}} = \begin{bmatrix} z_2 \\ z_3 \\ z_4 \\ a_x(z) \\ z_6 \\ z_7 \\ z_8 \\ a_y(z) \\ z_{10} \\ z_{11} \\ z_{12} \\ a_z(z) \\ z_{14} \\ a_\psi(z) \end{bmatrix} + \begin{bmatrix} \mathbf{0}_{3\times 4} \\ b_x(z) \\ \mathbf{0}_{3\times 4} \\ b_y(z) \\ \mathbf{0}_{3\times 4} \\ b_z(z) \\ \mathbf{0}_{1\times 4} \\ b_\psi(z) \end{bmatrix} \begin{bmatrix} \bar{u}_1 \\ u_2 \\ u_3 \\ u_4 \end{bmatrix}, \tag{17}$$

where

$$\begin{cases} \begin{bmatrix} a_x(z) \\ a_y(z) \\ a_z(z) \end{bmatrix} = \underbrace{\begin{pmatrix} -\frac{\varrho S(\boldsymbol{R_\Theta} e_3)\boldsymbol{R_\Theta} \boldsymbol{I}_B^{-1} S(\omega)\boldsymbol{I}_B \omega}{m} \\ -\frac{\boldsymbol{R_\Theta} S(\dot{\boldsymbol{\Theta}})^2 e_3 \varrho}{m} - \frac{2\boldsymbol{R_\Theta} S(\dot{\boldsymbol{\Theta}}) e_3 \varsigma}{m} \end{pmatrix}}_{3\times 1} \\ \begin{bmatrix} b_x(z) \\ b_y(z) \\ b_z(z) \end{bmatrix} = \begin{bmatrix} \underbrace{-\frac{\boldsymbol{R_\Theta} e_3}{m}}_{3\times 1} & \underbrace{\frac{\varrho S(\boldsymbol{R_\Theta} e_3)\boldsymbol{R_\Theta} \boldsymbol{I}_B^{-1}}{m}}_{3\times 3} \end{bmatrix} \\ a_\psi(z) = [\dot{\boldsymbol{T}}(\boldsymbol{\Theta})\omega - \boldsymbol{T}(\boldsymbol{\Theta})\boldsymbol{I}_B^{-1} S(\omega)\boldsymbol{I}_B \omega]_3 \\ b_\psi(z) = \begin{bmatrix} \mathbf{0}_{3\times 1} & \underbrace{\boldsymbol{T}(\boldsymbol{\Theta})\boldsymbol{I}_B^{-1}}_{3\times 3} \end{bmatrix}_3 . \end{cases} \tag{18}$$

Here $S(\omega)$ is the skew-symmetric matrix of ω such that $\dot{\boldsymbol{R}}_{\boldsymbol{\Theta}} = \boldsymbol{R_\Theta} S(\omega)$ and $S(\dot{\boldsymbol{\Theta}})$ is the skew-symmetric matrix of $\dot{\boldsymbol{\Theta}}$ which describe the Euler angle rates in $\mathcal{F}_W$. The subscript 3 in $a_\psi(z)$ and $b_\psi(z)$ means that only the third row of the expression is selected. The system equations expressed in z and $\bar{\boldsymbol{u}}$ are

$$\begin{bmatrix} \dddot{\boldsymbol{p}} \\ \ddot{\psi} \end{bmatrix} = \begin{bmatrix} \dddot{x} \\ \dddot{y} \\ \dddot{z} \\ \ddot{\psi} \end{bmatrix} = \begin{bmatrix} \dot{z}_4 \\ \dot{z}_8 \\ \dot{z}_{12} \\ \dot{z}_{14} \end{bmatrix} = \underbrace{\begin{bmatrix} a_x(z) \\ a_y(z) \\ a_z(z) \\ a_\psi(z) \end{bmatrix}}_{\triangleq \boldsymbol{a}(\boldsymbol{z})} + \underbrace{\begin{bmatrix} b_x(z) \\ b_y(z) \\ b_z(z) \\ b_\psi(z) \end{bmatrix}}_{\triangleq \boldsymbol{b}(\boldsymbol{z})} \bar{\boldsymbol{u}}. \tag{19}$$

As clear from (16), the state of the new system includes the jerk, which in general is not directly measurable. Therefore, for control purpose it can be computed as

$$\ddot{\boldsymbol{p}} = -\frac{1}{m}\left(\boldsymbol{R_\Theta} S(\omega) e_3 \varrho + \boldsymbol{R_\Theta} e_3 \varsigma\right). \tag{20}$$

For the new system model representation given by (19) to hold, we take the following assumption:

Assumption 4: The roll and pitch angles ϕ and θ are limited to $(-\pi/2,\ \pi/2)$.

Assumption 4 ensures that the matrix $\boldsymbol{b}(\boldsymbol{z})$ in (19) is non-singular, because $\boldsymbol{T}(\boldsymbol{\Theta})$ in (18) is nonsingular, and always has $rank(\boldsymbol{b}(\boldsymbol{z})) = 4$, therefore being invertible.

C. Uncertainties

The model presented in (19) depicts the system without uncertainties. To incorporate the effect of inexact knowledge of the parameters and of disturbances, we consider that:

1) the quadrotor is subject to external disturbances $\boldsymbol{\zeta}$ that act w.r.t. the CoM as force and torque wrenches. The dynamic equation (19) becomes

$$\begin{bmatrix} \dddot{\boldsymbol{p}} \\ \ddot{\psi} \end{bmatrix} = \boldsymbol{a}(\boldsymbol{z}) + \boldsymbol{b}(\boldsymbol{z})(\bar{\boldsymbol{u}} + \boldsymbol{\zeta}); \tag{21}$$

2) only the dynamic parameters m, $\boldsymbol{I}_B$ are uncertain.

Following these assumptions the above model (21) becomes

$$\begin{aligned} \begin{bmatrix} \dddot{\boldsymbol{p}} \\ \ddot{\psi} \end{bmatrix} &= \boldsymbol{a}_n + \Delta\boldsymbol{a} + \boldsymbol{b}_n(\bar{\boldsymbol{u}} + \boldsymbol{\zeta}) + \Delta\boldsymbol{b}(\bar{\boldsymbol{u}} + \boldsymbol{\zeta}) = \\ &= \boldsymbol{a}_n + \boldsymbol{b}_n\boldsymbol{u} + \boldsymbol{\xi}, \end{aligned} \tag{22}$$

where

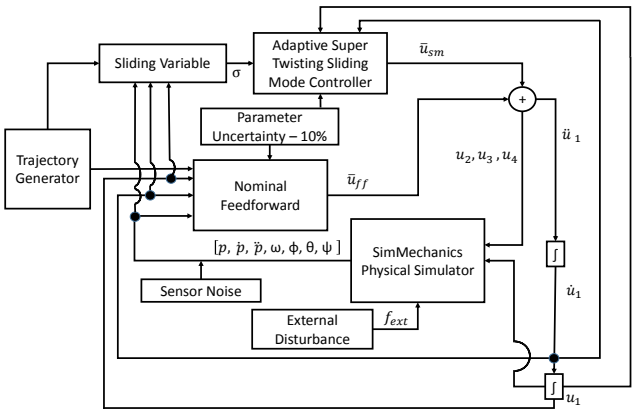

Fig. 1: Control scheme architecture. Jerk ($\dddot{\boldsymbol{p}}$) and snap ($\ddddot{\boldsymbol{p}}$) required in the adaptive controller and nominal feedback are calculated from acceleration ($\ddot{\boldsymbol{p}}$) of the quadrotor.

- $\boldsymbol{a}_n$ and $\boldsymbol{b}_n$ describe the nominal model of the robot;
- $\Delta\boldsymbol{a}$ and $\Delta\boldsymbol{b}$ contain the parametric uncertainties;
- $\boldsymbol{\xi} = \boldsymbol{b}_n\boldsymbol{\zeta} + \Delta\boldsymbol{a} + \Delta\boldsymbol{b}(\boldsymbol{u} + \boldsymbol{\zeta})$ is the vector of lumped perturbations.

Note that $\boldsymbol{b}_n$ is always full rank (Assumption 4), so the lumped perturbations satisfy the matching condition. Moreover, we make an additional assumption:

Assumption 5: $\boldsymbol{\xi}$ is bounded as $\|\boldsymbol{\xi}\|_2 \leq \xi_{\max}$, but the bound $\xi_{\max} \geq 0$ is unknown.

In practice it is difficult to estimate the upper bound on $\boldsymbol{\xi}$. This could lead to over-conservative gain tuning and consequently to unnecessary high control actions, chattering and noise amplification. Finally, we want to underline that we consider the case that only the dynamic parameters are uncertain.

III. CONTROL

In this section we propose our solution for trajectory tracking using a quadrotor in the presence of the lumped disturbance $\boldsymbol{\xi}$. The trajectory is specified as a desired position $\boldsymbol{p}_d(t) = \begin{bmatrix} x_d & y_d & z_d \end{bmatrix}^T$ with its derivatives up to the snap $\ddddot{\boldsymbol{p}}_d(t)$, and desired yaw ψ_d and its derivatives up to the second order $\ddot{\psi}_d$. Such a trajectory can be easily defined offline or computed online using input shaping or filtering techniques. We assume that the state variables defined in (16) are available at every time instant.

The tracking controller is designed as a robust law $\bar{\boldsymbol{u}}$ of the form

$$\bar{\boldsymbol{u}} = \bar{\boldsymbol{u}}_{sm} + \bar{\boldsymbol{u}}_{ff}, \tag{23}$$

where

- $\bar{\boldsymbol{u}}_{sm}$ is a term based on a sliding mode approach;
- $\bar{\boldsymbol{u}}_{ff}$ is a feedforward term based on the dynamic inversion of the nominal model.

In order to compute $\boldsymbol{u}$ from $\bar{\boldsymbol{u}}$, we need to double integrate u_1. In the remaining of this section we detail the two terms that compose $\bar{\boldsymbol{u}}$ in (23).

A. Adaptive Super Twisting Control

The sliding mode control term $\bar{\boldsymbol{u}}_{sm}$ is designed to steer to zero the tracking errors of position $\boldsymbol{e_p} = \boldsymbol{p} - \boldsymbol{p}_d = \begin{bmatrix} e_x & e_y & e_z \end{bmatrix}^T \in \mathbb{R}^3$ and yaw error $e_\psi = \psi - \psi_d$ in presence of the uncertainties $\boldsymbol{\xi}$. As seen earlier in Sec. II-B, in the model in regular form (19), the output is decoupled. Therefore, the sliding variable is chosen as

$$\boldsymbol{\sigma} = \begin{bmatrix} \sigma_x \\ \sigma_y \\ \sigma_z \\ \sigma_\psi \end{bmatrix} = \begin{bmatrix} \dddot{e}_x + \lambda_{x_3}\ddot{e}_x + \lambda_{x_2}\dot{e}_x + \lambda_{x_1}e_x \\ \dddot{e}_y + \lambda_{y_3}\ddot{e}_y + \lambda_{y_2}\dot{e}_y + \lambda_{y_1}e_y \\ \dddot{e}_z + \lambda_{z_3}\ddot{e}_z + \lambda_{z_2}\dot{e}_z + \lambda_{z_1}e_z \\ \dot{e}_\psi + \lambda_{\psi_1}e_\psi \end{bmatrix}, \tag{24}$$

where $\lambda \in \mathbb{R}^{n\times n}$ is a positive definite diagonal matrix. Using (19), the time derivative of $\boldsymbol{\sigma}$ is

$$\dot{\boldsymbol{\sigma}} = \begin{bmatrix} -\ddddot{x}_d + \lambda_{x_3}\dddot{e}_x + \lambda_{x_2}\ddot{e}_x + \lambda_{x_1}\dot{e}_x \\ -\dddot{y}_d + \lambda_{y_3}\dddot{e}_y + \lambda_{y_2}\ddot{e}_y + \lambda_{y_1}\dot{e}_y \\ -\dddot{z}_d + \lambda_{z_3}\dddot{e}_z + \lambda_{z_2}\ddot{e}_z + \lambda_{z_1}\dot{e}_z \\ -\ddot{\psi}_d + \lambda_{\psi_1}\dot{e}_\psi \end{bmatrix} + \boldsymbol{a}(\boldsymbol{z}) + \boldsymbol{b}(\boldsymbol{z})\bar{\boldsymbol{u}} \tag{25}$$

showing that $\boldsymbol{\sigma}$ has relative degree one with respect to $\bar{\boldsymbol{u}}$. To achieve the 2-sliding mode $\boldsymbol{\sigma} = \dot{\boldsymbol{\sigma}} = \boldsymbol{0}$, we implement $\bar{\boldsymbol{u}}_{sm}$ according to the well known Super Twisting controller (STC) [12], [17]. The expression of the standard STC is

$$\begin{aligned} \bar{\boldsymbol{u}}_{sm} &= \boldsymbol{b}(\boldsymbol{z})^{-1}\left(-\boldsymbol{\alpha}\,|\boldsymbol{\sigma}|^{\frac{1}{2}}\,sign(\boldsymbol{\sigma}) + \boldsymbol{v}\right) \\ \dot{\boldsymbol{v}} &= \begin{cases} -\bar{\boldsymbol{u}}_{sm} & \text{if } |\bar{\boldsymbol{u}}_{sm}| > \bar{\boldsymbol{u}}_m \\ -\boldsymbol{\beta}sign(\boldsymbol{\sigma}) & \text{if } |\bar{\boldsymbol{u}}_{sm}| \leq \bar{\boldsymbol{u}}_m \end{cases}. \end{aligned} \tag{26}$$

Here, $\bar{\boldsymbol{u}}_m$ denotes an upper bound for $\bar{\boldsymbol{u}}_{sm}$ and $\boldsymbol{\alpha}$, $\boldsymbol{\beta}$ are definite positive diagonal matrices of gains. The control law (26) has two remarkable properties, i) it does not require the knowledge of $\dot{\boldsymbol{\sigma}}$ and therefore of the snap $\ddddot{\boldsymbol{p}}$ and yaw acceleration $\ddot{\psi}$, and ii) the discontinuous function $sign(\boldsymbol{\sigma})$ is integrated, thus significantly attenuating chattering.

From [12] it is proved that the standard STC controller achieves finite-time convergence to the 2^{nd}order-sliding manifold with few assumptions. In particular, it is necessary to choose the gains $\boldsymbol{\alpha}$ and $\boldsymbol{\beta}$ high enough, according to the upper bound on $\boldsymbol{\xi}$. Since the upper bound on $\boldsymbol{\xi}$ is not known (Assumption 5) we adapt the gains online according to the law proposed in [1], [18],

$$\begin{aligned} \dot{\boldsymbol{\alpha}} &= \begin{cases} \boldsymbol{\omega}_{\boldsymbol{\alpha}}\sqrt{\dfrac{\gamma}{2}}\,sign\left(|\boldsymbol{\sigma}| - \boldsymbol{\mu}\right), & \text{if } \boldsymbol{\alpha} > \boldsymbol{\alpha}_m \\ \boldsymbol{\eta}, & \text{if } \boldsymbol{\alpha} \leq \boldsymbol{\alpha}_m \end{cases} \\ \boldsymbol{\beta} &= 2\,\epsilon\,\boldsymbol{\alpha}\,, \end{aligned} \tag{27}$$

where

- $\boldsymbol{\omega}_{\boldsymbol{\alpha}}, \gamma, \boldsymbol{\eta}$ are arbitrary positive constants;
- $\boldsymbol{\alpha}_m$ is an arbitrary small positive constant introduced to keep the gains positive;
- $\boldsymbol{\mu}$ is a positive parameter that defines the boundary layer for the real sliding mode.

Under few mild assumptions [1], the STC with adaptive gains (27) achieves finite-time convergence to a real 2-sliding mode $\|\boldsymbol{\sigma}\| \leq \boldsymbol{\mu}_1$ and $\|\boldsymbol{\sigma}\| \leq \boldsymbol{\mu}_2$, with $\boldsymbol{\mu}_1 \geq \boldsymbol{\mu}$ and $\boldsymbol{\mu}_2 \geq \boldsymbol{0}$.

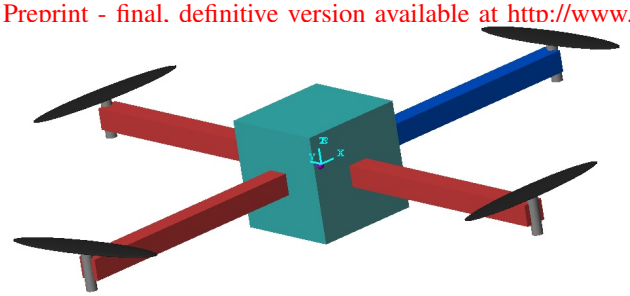

Fig. 2: Physical quadrotor model constructed in SimMechanics.

Note that the choice of the parameter $\boldsymbol{\mu}$ in (27) is critical. A wrong choice of this parameter could lead to either instability and the control gains shooting up to infinity or to poor accuracy [2]. Here, we choose $\boldsymbol{\mu}$ as a time-varying parameter function according to [2]. Therefore $\boldsymbol{\mu}$ is given by

$$\boldsymbol{\mu}(t) = 4\,\boldsymbol{\alpha}(t)\,T_e\ , \tag{28}$$

where T_e is the sampling time for the controller.

An important remark on (27) is that the gain adaptation law does not need any knowledge of the upper bound of the external perturbations $\boldsymbol{\xi}$. Moreover, the gains $\boldsymbol{\alpha}$ and $\boldsymbol{\beta}$ are not chosen according to a worst case uncertainty, but rather they are increased only when necessary. This further reduces the chattering in the ASTC.

B. Feedforward Control

The feedforward component $\bar{\boldsymbol{u}}_{ff}$ based on the dynamic inversion of the nominal model from (23) is the wrench that needs to be applied to the nominal model of the UAV to track a reference trajectory, in the absence of initial error. The $\bar{\boldsymbol{u}}_{ff}$ part of the control wrench decreases the magnitude of sliding mode control $\bar{\boldsymbol{u}}_{sm}$, thus helping in reducing the gains of the ASTC and hence attenuates chattering. The expression of $\bar{\boldsymbol{u}}_{ff}$ is obtained by dynamic inversion of (19) as

$$\bar{\boldsymbol{u}}_{ff} = \boldsymbol{b}\,(\boldsymbol{z})^{-1}\left(\begin{bmatrix}\dddot{x}_d\\ \dddot{y}_d\\ \dddot{z}_d\\ \ddot{\psi}_d\end{bmatrix} - \boldsymbol{a}\,(\boldsymbol{z})\right)\ . \tag{29}$$

Figure 1 shows the control scheme architecture of the developed controller.

IV. PHYSICAL SIMULATIONS

The quadrotor model (19), reformulated with the change of coordinates in (16), and the capability of the developed adaptive super twisting controller defined by (26) and (27) are extensively verified by means of physical simulations. We have built a quadrotor system model in SimMechanics[1] using joints, constraints and force elements. SimMechanics formulates and solves the equations of motion for the complete 3D mechanical multibody system and is interfaced with the Matlab/Simulink environment for rapid control design and implementation.

[1]http://www.mathworks.com/products/simmechanics/

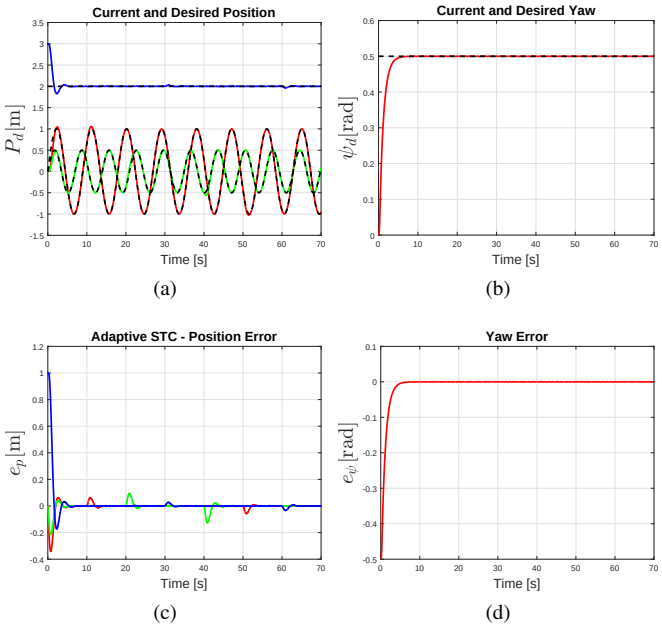

Fig. 3: Results of robust trajectory tracking for position $\boldsymbol{p}$ and yaw ψ. 3(a): Desired (dashed black line) and current (solid line) position $\boldsymbol{p}_d$ in x (red), y (green) and z (blue). 3(b): Desired (dashed line) and current (solid line) yaw (red) $\boldsymbol{\psi}_d$. 3(c–d): behavior of the position/orientation tracking errors ($\boldsymbol{e}_p$, $\boldsymbol{e}_\psi$).

Our aim in this simulation is (i) to prove the robustness of the developed ASTC, (ii) to demonstrate the ability to perform aggressive trajectory tracking maneuvers and (iii) to compare it with standard STC. In the rest of this section we provide a brief description of the experimental setup (Sec. IV-A), we show and discuss simulation results of ASTC during aggressive maneuver trajectory tracking (Sec. IV-B) and we compare in detail the ASTC with the standard STC (Sec. IV-C).

A. Experimental Setup

The physical quadrotor model in SimMechanics, shown in Fig. 2, is designed using the parameters of a real quadrotor with total mass $m = 2.6Kg$ and inertial parameters $\boldsymbol{I}_B = \begin{bmatrix}Ixx & Iyy & Izz\end{bmatrix}^T = \begin{bmatrix}0.0488 & 0.0488 & 0.0956\end{bmatrix}^T Kg\cdot m^2$. Note that in the control law these parameters will be considered uncertain. The other system parameters, the lift coefficient b, the drag coefficient d and the arm length l, are considered to be known without uncertainty. The system state, namely the position $\boldsymbol{p} = \begin{bmatrix}x & y & z\end{bmatrix}^T$, linear velocity $\dot{\boldsymbol{p}} = \begin{bmatrix}\dot{x} & \dot{y} & \dot{z}\end{bmatrix}^T$, acceleration $\ddot{\boldsymbol{p}} = \begin{bmatrix}\ddot{x} & \ddot{y} & \ddot{z}\end{bmatrix}^T$ in $\mathcal{F}_W$ and the angular velocity $\boldsymbol{\omega_B} = \begin{bmatrix}p & q & r\end{bmatrix}^T$ in $\mathcal{F}_B$ are provided to the controller as noisy measurements, with an additional gaussian noise to resemble realistic measurements from an external tracking system and an onboard IMU.

B. Robustness of ASTC

The desired quadrotor trajectory $\boldsymbol{p}_d$ provided as reference to the controller is a sinusoid along the X and Y axes. The highly aggressive nature of the trajectory is highlighted by

the roll and pitch angles during the tracking that reaches up to $\pm 20°$. In order to highlight the robust nature of the controller, the initial position error is set to $\boldsymbol{p}_e = \begin{bmatrix} 0 & 0 & 1 \end{bmatrix}^T m$. Additionally, during the execution of the trajectory, the quadrotor is subjected to high force disturbance in all the principal axes ($f_{\text{ext}_x} = 2N$, $f_{\text{ext}_y} = 3N$ and $f_{\text{ext}_z} = 1N$) which are applied and removed at different time instants, as shown in Fig. 4(a). Furthermore, a parameter uncertainty of 10% is included in the controller for the mass m and inertial matrix $\boldsymbol{I}_B$. Therefore this simulation aims to prove the robustness, asymptotic trajectory tracking and stability performance of the controller in presence of initial error, noisy system state, parameter uncertainty and external disturbance.

Figure 3(a) shows the desired position $\boldsymbol{p}_d$ and the current position $\boldsymbol{p}$. Figure 3(b) shows the desired yaw ψ_d and the current yaw ψ along with the yaw error e_ψ in Fig. 3(d). As seen from tracking error $\boldsymbol{e}_p$ in Fig. 3(c), the controller shows asymptotic stability even when many nonidealities are are introduced in the model.

Figure 4(a) displays the external force disturbance $\boldsymbol{f}_{ext}$ applied on the quadrotor in all the principal axes. The sliding variable $\boldsymbol{\sigma}$, shown in Fig. 4(b), $\boldsymbol{\sigma}$ varies with high frequency because of the noise affecting the system state. Figure 4(c) shows the adaptation of the $\boldsymbol{\alpha}$ gain given by (27). Comparing Fig. 4(a) and Fig. 4(c), it is possible to notice the spikes in the α gains, due to their adaptation when the disturbance forces are applied or removed. A similar behavior can be observed in the nominal feedforward input computed using (29) and shown in Fig. 4(d). The control input $\boldsymbol{u}$ and the gain adaptation of $\boldsymbol{\alpha}$ are discussed in detail in Sec. IV-C.

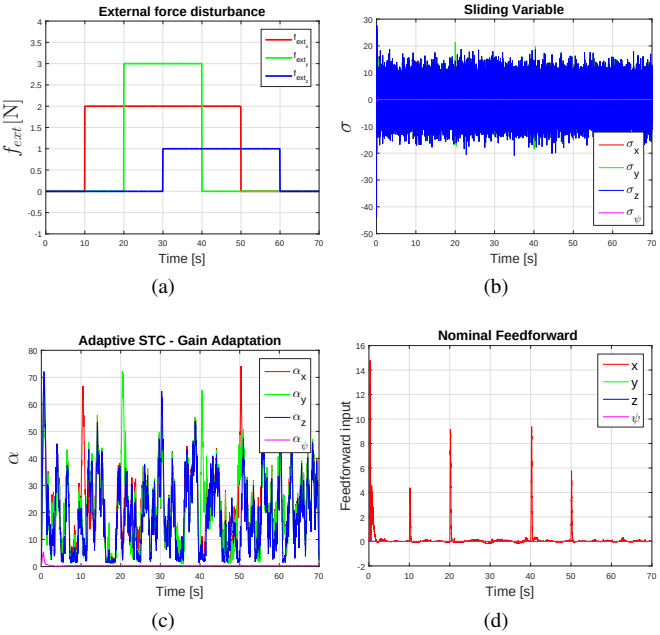

(a) (b) (c) (d)

Fig. 4: Results from ASTC. 4(a): External disturbance $\boldsymbol{f}_{ext}$ applied on the quadrotor in f_{ext_x} (red), f_{ext_y} (green) and f_{ext_z} (blue). 4(b): Sliding variable $\boldsymbol{\sigma}$ in σ_x (red), σ_y (green), σ_z (blue) and σ_ψ (magenta). 4(c): Adaptive $\boldsymbol{\alpha}$ gain of ASTC in α_x (red), α_y (green), α_z (blue) and α_ψ (magenta). 4(d): Nominal feedforward proposed in ASTC as ff_x (red), ff_y (green), ff_z (blue) and ff_ψ (magenta)

C. Comparison of ASTC and STC

The same physical simulation described in Sec. IV-B is performed also for the standard version of the super twisting controller (STC). Figure 5 shows thrust ρ, roll torque τ_x, pitch torque τ_y and yaw torque τ_z computed in the two simulations. It is clear from Fig. 5(b) that the control inputs computed by the standard STC are affected by continuous chattering, whereas Fig. 5(a) shows that the chattering is substantially reduced and is only present when the gains are adapting to high values to counterbalance the external force disturbance $\boldsymbol{f}_{\text{ext}}$.

Figure 6 shows the position error $\boldsymbol{e_p}$ of the ASTC and STC. Clearly, the chattering on the control inputs reflects in a noisy tracking of the desired trajectory (Fig. 6(b)), while the ASTC controller shows a smoother behavior (Fig. 6(a)). The big difference between the ASTC and standard STC is due to the adaptation of the $\boldsymbol{\alpha}$ gain: while the gains of the STC are constant fixed to $\left(\begin{bmatrix} \alpha_x & \alpha_y & \alpha_z & \alpha_\psi \end{bmatrix} = \begin{bmatrix} 20 & 20 & 20 & 2 \end{bmatrix}\right)$, the gains of the ASTC are able to vary as shown in Fig. 4(c). The interested reader is invited to see the video of the physical simulations included as part of this work.

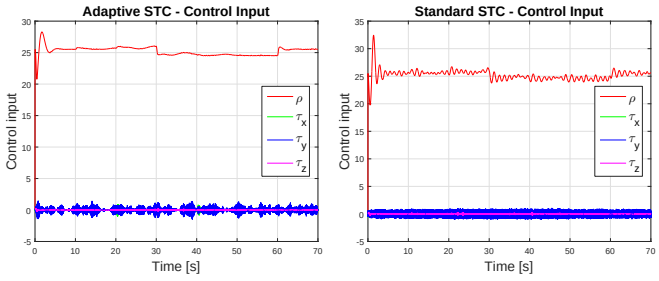

(a) (b)

Fig. 5: Results of the thrust and torque control inputs that are given to the quadrotor. 5(a): thrust ρ (red), roll torque τ_x (green), pitch torque τ_y (blue) and yaw torque τ_z (magenta) with ASTC. 5(b): thrust ρ (red), roll torque τ_x (green), pitch torque τ_y (blue) and yaw torque τ_z (magenta) with standard STC.

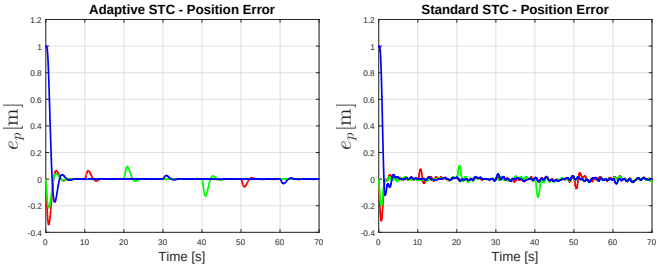

(a) (b)

Fig. 6: Results of the position tracking error $\boldsymbol{e_p}$ for aggressive maneuvers. 6(a): e_x (red), e_y (green), e_z (blue) using ASTC. 6(b): e_x (red), e_y (green), e_z (blue) using standard STC.

V. CONCLUSIONS

In this paper we have considered the problem of trajectory tracking with a quadrotor UAV in presence of uncertainties, external wrenches and noise on the measurements. We have implemented a robust controller based on a Super Twisting architecture with adaptive gains. The controller is also extended to include a feedforward dynamic inversion of the nominal model. The main features of the proposed method are (i) the knowledge of the upper bound of the perturbations is not needed and (ii) chattering is limited. Physical Simulations show that the controller is effective, even in comparison to a recently proposed super twisting controller. In the future, we plan to continue this work by implementing the controller on a real quadrotor and running extensive experiments.

REFERENCES

[1] Y. B. Shtessel, M. Taleb, and F. Plestan, "A novel adaptive-gain supertwisting sliding mode controller: Methodology and application," vol. 48, no. 5, pp. 759–769, 2012.

[2] F. Plestan, Y. Shtessel, V. Brégeault, and A. Poznyak, "New methodologies for adaptive sliding mode control," vol. 83, no. 9, pp. 1907–1919, 2010.

[3] M. Orsag, C. Korpela, and P. Oh, "Modeling and control of mm-uav: Mobile manipulating unmanned aerial vehicle," *Journal of Intelligent and Robotic Systems*, vol. 69, no. 1-4, pp. 227–240, 2013.

[4] V. Lippiello and F. Ruggiero, "Exploiting redundancy in cartesian impedance control of uavs equipped with a robotic arm," in *Intelligent Robots and Systems (IROS), 2012 IEEE/RSJ International Conference on*, Oct 2012, pp. 3768–3773.

[5] P. E. I. Pound, D. R. Bersak, and A. M. Dollar, "Grasping from the air: Hovering capture and load stability," in *2011*, 2011, pp. 2491–2498.

[6] Q. Lindsey, D. Mellinger, and V. Kumar, "Construction of cubic structures with quadrotor teams," 2011.

[7] G. Gioioso, M. Ryll, D. Prattichizzo, H. Bülthoff, and A. Franchi, "Turning a near-hovering controlled quadrotor into a 3d force effector," in *Robotics and Automation (ICRA), 2014 IEEE International Conference on*, May 2014, pp. 6278–6284.

[8] B. Yüksel, C. Secchi, H. H. Bülthoff, and A. Franchi, "Reshaping the physical properties of a quadrotor through ida-pbc and its application to aerial physical interaction," in *2014 IEEE Int. Conf. on Robotics and Automation*, Hong Kong, China, May 2014, pp. 6258–6265.

[9] V. Mistler, A. Benallegue, and N. M'Sirdi, "Exact linearization and noninteracting control of a 4 rotors helicopter via dynamic feedback," in *Robot and Human Interactive Communication, 2001. Proceedings. 10th IEEE International Workshop on*, 2001, pp. 586–593.

[10] D. Lee, H. Jin Kim, and S. Sastry, "Feedback linearization vs. adaptive sliding mode control for a quadrotor helicopter," *International Journal of Control, Automation and Systems*, vol. 7, no. 3, pp. 419–428, 2009.

[11] L. Derafa, L. Fridman, A. Benallegue, and A. Ouldali, "Super twisting control algorithm for the four rotors helicopter attitude tracking problem," in *Variable Structure Systems (VSS), 2010 11th International Workshop on*, June 2010, pp. 62–67.

[12] Y. Shtessel, C. Edwards, L. Fridman, and A. Levant, *Sliding Mode Control and Observation*, 2014.

[13] H. Bouadi, S. Simoes Cunha, A. Drouin, and F. Mora-Camino, "Adaptive sliding mode control for quadrotor attitude stabilization and altitude tracking," in *Computational Intelligence and Informatics (CINTI), 2011 IEEE 12th International Symposium on*, Nov 2011, pp. 449–455.

[14] H. Castaneda, O. Salas-Pena, and J. de Leon Morales, "Adaptive super twisting flight control-observer for a fixed wing uav," in *Unmanned Aircraft Systems (ICUAS), 2013 International Conference on*, May 2013, pp. 1004–1013.

[15] D. Lee, A. Franchi, H. I. Son, C. Ha, H. Bülthoff, and P. Giordano, "Semiautonomous haptic teleoperation control architecture of multiple unmanned aerial vehicles," *Mechatronics, IEEE/ASME Transactions on*, vol. 18, no. 4, pp. 1334–1345, Aug 2013.

[16] A. Isidori, *Nonlinear Control Systems, 3rd edition*, 1995.

[17] A. Levant, "Sliding order and sliding accuracy in sliding mode control," vol. 58, no. 6, pp. 1247–1263, 1993.

[18] Y. B. Shtessel, J. A. Moreno, F. Plestan, L. Fridman, and A. S. Poznyak, "Super-twisting adaptive sliding mode control: A Lyapunov design," in *2010*, Dec 2010, pp. 5109–5113.